

# Palm Frond and Spikelet as Environmentally Benign Alternative Solid Acid Catalysts for Biodiesel Production

Yahaya M. Sani,<sup>a,b</sup> Aisha O. Raji,<sup>b</sup> Peter A. Alaba,<sup>a</sup> A. R. Abdul Aziz,<sup>a</sup> and Wan Mohd A. Wan Daud<sup>a,\*</sup>

A carbonization-sulfonation method was utilized in synthesizing sulfonated mesoporous catalysts from palm tree biomass. Brunauer-Emmet-Teller (BET), powder X-ray diffraction (XRD), energy dispersive X-ray (EDX), and field emission scanning emission microscopy (FE-SEM) analyses were used to evaluate the structural and textural properties of the catalysts. Further, Fourier transform infrared (FT-IR) spectroscopy and titrimetric analyses measured the strong acid value and acidity distribution of the materials. These analyses indicated that the catalysts had large mesopore volume, large surface area, uniform pore size, and high acid density. The catalytic activity exhibited by esterifying used frying oil (UFO) containing high (48%) free fatty acid (FFA) content further indicated these properties. All catalysts exhibited high activity, with sPTS/400 converting more than 98% FFA into fatty acid methyl esters (FAMEs). The catalyst exhibited the highest acid density, 1.2974 mmol/g, determined by NaOH titration. This is outstanding considering the lower reaction parameters of 5 h, 5:1 methanol-to-oil ratio, and a moderate temperature range between 100 and 200 °C. The study further illustrates the prospect of converting wastes into highly efficient, benign, and recyclable solid acid catalysts.

*Keywords:* Biomass; Mesoporous carbon sulfonation; Solid acid catalyst; High free fatty acid; Esterification

*Contact information:* a: Department of Chemical Engineering, University of Malaya, 50603 Kuala Lumpur, Malaysia; b: Department of Chemical Engineering, Ahmadu Bello University, 870001, Nigeria;

\* Corresponding author: ashri@um.edu.my

## INTRODUCTION

Despite the recent fall in the price of Brent crude oil, the search for a sustainable and ecologically benign alternative persists. This is due to the pollution caused by crude oil exploration and the combustion of refined oil products (Sani *et al.* 2013; Hassan *et al.* 2015), coupled with weaker demand for petroleum fuels. One alternative being aggressively researched is the transesterification of triglycerides (TG) with methanol into biodiesel or fatty acids methyl esters (FAME) (Ghadge and Raheman 2006). However, feedstocks for this process containing large amounts of free fatty acids (FFAs), such as used frying oil (UFO), animal fats, and vegetable oils, usually incur postproduction costs in soap separation after alkali-catalyzed transesterification. This substantially decreases the biodiesel yield (Park *et al.* 2010). Reducing the FFA content of these feedstocks to approximately 1% (acid value of less than 2 mg KOH/g) is necessary before transesterification (Lotero *et al.* 2005; Zhang and Jiang 2008).

Similarly, there are several drawbacks to the two-step process of acid-catalyzed pre-esterification of FFA into esters with H<sub>2</sub>SO<sub>4</sub> followed by alkali-catalyzed transesterification (Ramadhas *et al.* 2005; Ghadge and Raheman 2006; Veljkovic *et al.*

2006; Wang *et al.* 2006; Berchmans and Hirata 2008; Zhang and Jiang 2008). These include equipment corrosion, difficulty in product separation from homogeneous mixtures, non-recyclability of the catalysts, and high-energy consumption during purification (Sani *et al.* 2012). These highlight the increasingly urgent need for affordable acid catalysts with good catalytic performance that could alleviate the mentioned issues.

The discovery of sugar catalysts showed that carbon-based solid acids are promising alternatives to homogeneous alkaline and liquid acid catalysts (Toda *et al.* 2005). Recently, incorporating  $-SO_3H$  *via* the carbonization-sulfonation method into carbon biomass sources such as cellulose, corn straw, starch, glucose, and sucrose (Zhang *et al.* 2015; Lou *et al.* 2008) has exhibited good catalytic performance during esterification (Toda *et al.* 2005; Takagaki *et al.* 2006; Budarin *et al.* 2007; Zong *et al.* 2007; Agulló *et al.* 2010; Dehkhoda *et al.* 2010; Maciá-Liu *et al.* 2013) in spite of their low surface area and porosity, which limit reactant diffusion to active sites (Zhang *et al.* 2015). However, numerous groups have recently synthesized sulfonated, ordered, mesoporous carbons *via* nanocasting with SBA-15 as a template and phenolic resol and Pluronic F127 self-assemblies under acidic conditions, respectively (Wang *et al.* 2007; Xing *et al.* 2007; Liu *et al.* 2008; Peng *et al.* 2010; Janaun and Ellis 2011; Sukanuma *et al.* 2011; Geng *et al.* 2012). Similarly, Peng *et al.* (2005) and Yu *et al.* (2008) describe how to prepare catalysts for esterification *via* the high temperature sulfonation of carbon nanotubes. The acidity, large pore size, and high surface area of these materials ensure accessibility of long-chain FFA molecules and high catalytic activity. However, a literature survey revealed that no reports are available regarding acid-catalyzed reactions using palm tree biomass.

Developing efficient solid catalysts from low-value biomass is essential to making the process ecologically friendly and economical. Malaysia, the world's second largest producer and exporter of palm oil, generates a deluge of biomass from oil palm production. According to Sulaiman *et al.* 2012, oil palm production generates 85.5% of the total biomass produced from a variety of crops, including but not limited to rubber, rice, and oil palm. This accounts for the highest percentage with little to no economic value.

These include palm trunks, palm mesocarp fibre (PMF), empty fruit bunches (EFB), palm fronds, spikelets, and kernel shells (PKS) (Hassan *et al.* 1997; Aziz *et al.* 2011). Incidentally, agricultural residues from renewable sources, which are both abundant and inexpensive, can serve as remarkable feedstocks for fuel production and catalyst development (Prauchner and Rodríguez-Reinoso 2012). Incidentally, the availability of oil palm frond and spikelets is increasing. According to data obtained from <http://www.bfdic.com/en/Features/Features/79.html>, 75 to 80% of emptied fruit bunch is spikelets while the main stalk makes up the remaining 20 to 25%. An estimated average of 2.856 million tonnes (dry basis) of empty fruit bunches will be produced per year from 2007 to 2020 from the current and expanding planting area of ca. 4.0 million hectares. Similarly, an estimated 10.4 tonnes  $ha^{-1}$  of fronds equates to an average of 6.97 and 54.43 million tonnes per year during pruning activity and replanting process respectively, within the same period. Further, it is important to highlight that despite the mass production, only ca. 10% of the total biomass produced is made of oil. It is therefore necessary to transform the remaining large amount of waste biomass to useful resources.

This paper demonstrates the synthesis of sulfonated, mesoporous carbon catalysts with concentrated  $H_2SO_4$  (98%) as the sulfonating reagent and palm tree frond and spikelet from oil palm (*Elaeis guineensis*) as the carbon precursors. The study investigated the effects of the resultant catalysts in simultaneously esterifying FFA into FAME.

## Materials and Catalyst Preparation

Room-temperature drying for one week ensured steady moisture loss from the oil palm residues (fronds and spikelets). This was measured using the oven-dry basis mass, OD (Eq. 1) before oven drying at 120 °C for 24 h followed by milling and sieving (mesh size, 0.5 mm). Catalyst preparation was done according to a modified procedure previously documented (Toda *et al.* 2005; Dawodu *et al.* 2014). Low-temperature, incomplete carbonization induced polycyclic aromatic carbon ring formation from cellulosic palm residues. Heating the dried powder in a tubular furnace at 400 °C, with temperature increasing at 2 °C/min, for 24 h under a nitrogen (N<sub>2</sub>) atmosphere produced incompletely carbonized materials. Treatment with concentrated sulfuric acid introduced sulfonite groups (-SO<sub>3</sub>H) into the material. This was done by heating the solids (20 g) in 200 cm<sup>3</sup> of concentrated H<sub>2</sub>SO<sub>4</sub> (98%) at 150 °C. Adding distilled water (1000 cm<sup>3</sup>) after heating for 10 h and then cooling the mixture to room temperature yielded a black precipitate. Washing the precipitate with hot distilled water (temperature above 80 °C) ensured the absence of impurities such as sulfate ions. The material was then oven dried at 70 °C before it was homogenized with succinic acid (SA). Mixing the carbon material (10 g) with 5 g of succinic acid and 40 cm<sup>3</sup> of de-ionized water, then heating at 150 °C for 5 h, achieved proper sulfonation. After filtering and washing with distilled water and methanol, oven-drying the resulting product at 100 °C for 5 h produced rigid carbon materials. The sulfonated palm fronds were designated sPTF/SA/T, where T denotes the carbonization temperature (300 or 400 °C). A non-homogenized reference material, designated sPTF/400, was synthesized to evaluate the effects of SA addition. Catalyst prepared from palm tree spikelet was designated sPTS/T without SA addition. These differences in reaction conditions helped to create the optimum sulfonated catalyst synthesized from oil palm residues for esterification.

Moisture content (%; OD basis) = (weight of water ÷ dry weight of wood) x 100 (1)

## Methods

### Catalyst characterization

A FEI QUANTA™ 450 FEG type 2033/14 (Czech Republic) unit with 30 kV accelerating voltage was used for field emission scanning electron microscopy (FE-SEM) to analyze the surface morphology and topology of the catalysts. An energy dispersive X-ray spectrometer (EDX) from the same unit revealed the surface elemental composition of the catalysts. Further, X-ray diffraction (XRD) and BET analyses were used to determine the structural and textural properties of the catalysts. The XRD patterns were analyzed with a Phillips X'pert diffractometer (The Netherlands) using CuK $\alpha$  radiation ( $\lambda = 1.54056 \text{ \AA}$ ) at a scanning speed of 0.05°/s within a  $2\theta$  range of 5 to 70° at 40 mA and 40 kV. Micromeritics TriStar II (USA) with accelerated surface area porosity (ASAP)-3020 at minus 196.15 °C was used to determine the specific surface area of the catalytic materials using liquid nitrogen. Degassing the catalysts at 120 °C for 3 h under a vacuum eliminated any physisorbed volatiles and impurities. Rapid (scan speed 3 velocities, 2.2 to 20 kHz) identification and quantification of the catalysts was performed with a Bruker Fourier transform infrared (FT-IR) Tensor 27 IR (Germany). The apparatus has a spectral range of 7500 to 370 cm<sup>-1</sup> with more than 1 cm<sup>-1</sup> apodized resolution and a standard KBr beam splitter.

### Production of fatty acid methyl esters

The catalysts were heated at 150 °C for 1 h before the reaction to evacuate adsorbed water and other volatiles. Methanol, with the aid of the catalyst, was used to transesterify used frying oil (UFO) at 100 to 200 °C in a 100 mL autoclave (250 °C, 100 bar) reactor supplied by AmAr Equipment Pvt., Ltd. (Mumbai). Constant stirring ensured contact between the catalyst and the reaction mixture. A reflux condenser attached to the autoclave maintained the temperature during the reaction. Preliminary optimization showed that a 5:1 methanol-to-oil molar ratio and 1 wt.% catalyst loading are optimal reaction conditions. Simple decanting was done to recover the FAME at the end of the 3 to 15 h reaction. Drying, methanol washing, and heating at 120 °C for 1 h regenerated the catalyst. The catalyst retained its activity after regeneration for up to 8 recycles.

### Acid density analysis

Exchanging Na<sup>+</sup> with H<sup>+</sup> in the form of -SO<sub>3</sub>H by mixing 0.1 g of sulfonated material with 30 mL of 0.6-M NaCl solution for 2 h facilitated determination of the acid strength of the catalysts. The filtrate from this mixture was titrated with 0.1001 M NaOH standard solution and methyl orange indicator to indicate when the NaOH was consumed. A change from slightly red to bright yellow maintained for 30 s was defined as the end point. To determine the initial, unconsumed volume of the NaOH standard solution, a blank titration was performed. Equation 2 was used to accurately calculate the strong acid (-SO<sub>3</sub>H) density.

$$D_{-SO_3H} = \frac{C_{OH^-} \times [V_1 - V_0]}{m_{cat.}} \quad (2)$$

The strong acid (-SO<sub>3</sub>H) density of the catalyst (in mmol/g) and the concentration of standard NaOH solution are represented by  $D_{-SO_3H}$  and  $C_{OH^-}$ , respectively. The volume of NaOH standard solution consumed during the blank and catalyst titrations are represented by  $V_0$  and  $V_1$ , respectively;  $m_{cat}$  represents the mass of catalyst used for the acid density analysis.

### Determination of Acid Value

The oil's acid value was determined by titration analysis according to DIN EN ISO 660 (2009). The expected acid value of used frying oil is between 15 and 75 mg KOH/g. The titrant, 0.1 M KOH, neutralizes the solvent mixture comprised of 50 mL of ethanol-diethyl ether (1:1 ratio, v/v) mixed with 0.5 g of catalyst sample. Equations 3, 4, and 5 were used to calculate the titre value, acid value, and FFA conversion, respectively,

$$\text{Titre value} = \frac{m_s}{V_{EP_1} \times c(KOH) \times M_A} \quad (3)$$

$$\text{Acid value} = \frac{V_{EP_1} \times f \times c(KOH) \times M_A}{m_s} \quad (4)$$

$$\text{FFA conversion, \%} = \frac{V_{EP_1} \times f \times c(KOH) \times M_A}{10 \times m_s} \quad (5)$$

where  $V_{EP_1}$  represents the titrant consumed at end of the first equivalent point in mL,  $c(KOH)$  represents the concentration of KOH titrant (0.1 M),  $M_A$  represents the molecular

weight of the analyte (112.12 g/mol),  $f$  represents the correction factor obtained from the titre value,  $M_A$  represents the molecular weight of palmitic acid (256 g/mol), and  $m_s$  represents the sample size in g.

## RESULTS AND DISCUSSION

### Characterization of Biomass

A previous study (Aziz *et al.* 2011) described the approximate oil palm biomass composition from oil palm (*Elaeis guineensis*) as 45 to 50% carbon, 43 to 48% oxygen, 0.5% nitrogen, 5% hydrogen, and 0.4% sulfur. Similarly, proximate analysis revealed that the oil palm biomass consisted of 72 to 75% volatile matter, 14 to 16% fixed carbon, 6 to 8% moisture, and 2 to 5% ash. Specifically, petiole, leaflets, and rachis are the three main parts of the palm fronds. The petiole consists of about 70% of the dry matter in the palm fronds, while the leaves and rachis make up the remaining percentage. The dry matter content of palm fronds is about 31% (Ishida and Abu Hassan 1992). Depending on age, palm fronds contains *ca.* 15 to 26% hemicellulose. It also contains 4.7 MJ/kg crude proteins, 38.5 MJ/kg crude fibre, 2.1 MJ/kg ether extract, 78.7 MJ/kg neutral-detergent fibre, and 3.2 MJ/kg ash (Wong and Wan Zahari 1997; Wan Zahari *et al.* 2000). Similarly, (Rabumi 1998) reported 70.9 to 90.1 C/N ratio, 25.0 to 29.9% lignin, 16.2 to 21.3% cellulose, 1.52 to 2.46% soluble polyphenols, as the chemical composition of spikelets.

A previous report by Chen *et al.* (2010) identified  $2\theta$  peaks ranging from  $22^\circ$  to  $23^\circ$  as the major diffraction peaks for cellulose crystallography. Figure 1 shows the small angle XRD pattern for all the samples. The figure displays one broad XRD peak at about a  $2\theta$  value of  $24^\circ$  with  $d$  value, calculated using the Bragg equations, of 3.86 nm. The noticeable peak confirmed the presence of crystallinity within the amorphous structure of the cellulosic constituents (Lai and Idris 2013). Further, Liu *et al.* (2012) posited the prominent  $I_{002}$  peak with the maximum intensity of 002 lattice diffraction as the primary as well as crystalline.

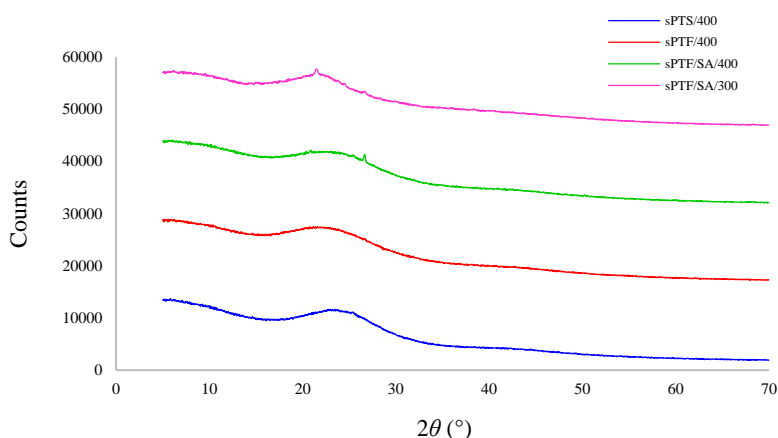


**Fig. 1.** Small angle XRD patterns of sPTS/400, sPTF/400, sPTF/SA/300, and sPTF/SA/400

The broad nature of the peak is reflective of the cellulosic molecular hydrogen bond transformation during heat treatment. However, the low crystallinity indicated the presence of larger amounts of amorphous cellulose in the catalytic materials (Kuo and Lee 2009). Certainly, from the representation on Fig. 1, one may recognize the correlation between

the good performance of sPTS/400 and the crystal structure. The material exhibited a spike at  $2\theta$  value of  $24^\circ$ , which falls within the range reported for cellulose crystallography by Chen *et al.* (2010). The next in line after sPTS/400 is sPTF/400 with a spike at  $2\theta$  value of  $25.44^\circ$  and a d-spacing of  $3.498\text{\AA}$ . Evidently, crystallinity and the total acid ( $-\text{SO}_3\text{H}$ ) density of these materials facilitated their observed catalytic performances over sPTF/SA-300 and sPTF/SA-400.

The  $\text{N}_2$  adsorption results presented in Table 1 and Fig. 2 confirmed the presence of mesopores ( $2 < dp < 50$  nm) on the prepared catalytic materials, consistent with aromatic sheets of amorphous carbon orientation. This was evidenced by the clear nitrogen condensation steps in Fig. 2. Further, Fig. 2 shows the  $\text{N}_2$  adsorption-desorption isotherm and pore size distribution curves of mesoporous carbon obtained at  $400^\circ\text{C}$  carbonization temperature. The pore size distribution curves of the two materials (with and without SA) show similar shapes with high pore size uniformity with a highly uniform pore diameter centered at about 17.8 nm. The large mesopores are advantageous because they minimize diffusion limitation and facilitate easier access to the reacting molecules to the active sites within the materials. Additionally, the large mesopores enhance the stability of the ordered mesoporous carbon framework (Zhang *et al.* 2015).

The adsorption isotherm of all samples followed a type-IV IUPAC classification for mesoporous materials with capillary condensation taking place at higher pressures of adsorbate depicting a hysteresis loop (Sing *et al.* 1985). At higher pressures, the slope showed increased uptake of adsorbate as pores become filled, with the inflection point typically occurring near completion of the first monolayer. The H<sub>4</sub>-type hysteresis loop fit well to the ink-bottle pores expected for the voids between the materials. At lower pressures, an adsorbate monolayer formed on the pore surface, which was followed by multilayer formation. However, it is interesting to note that mesoporosity alone did not determine the extent of catalytic activity or turnover. Other factors, such as acid sites and type, acid density, carbon precursor and crystal structure, all played significant roles.

Titrimetric, structural, and surface analyses revealed strong acid ( $-\text{SO}_3\text{H}$ ) densities (Table 1) and amorphous carbon sheets bearing hydroxyl ( $-\text{OH}$ ) and carboxyl ( $-\text{COOH}$ ) groups. Interestingly, the carbon catalysts remained insoluble even above the boiling temperatures of water, methanol, oleic acid, benzene, and hexane (Toda *et al.* 2005). Furthermore, the presence of low crystallinity also indicates the catalysts' affinity for anchoring  $-\text{SO}_3\text{H}$  groups.

**Table 1.** Surface Properties and Total Acid Density ( $-\text{SO}_3\text{H}$ ) of the Catalysts

Catalyst	Surface Area ( $\text{m}^2/\text{g}$ )	Pore Size (nm)	Pore Volume ( $\text{cm}^3/\text{g}$ )	Total Acid ( $-\text{SO}_3\text{H}$ ) Density ( $\text{mmol}/\text{g}$ )
sPTF/SA/400	28.1057	10.1712	0.033078	0.7851
sPTF/SA/300	27.7805	10.0154	0.030178	1.1283
sPTF/400	17.8048	9.1975	0.028308	1.0873
sPTS/400	12.7037	5.1565	0.019907	1.2974

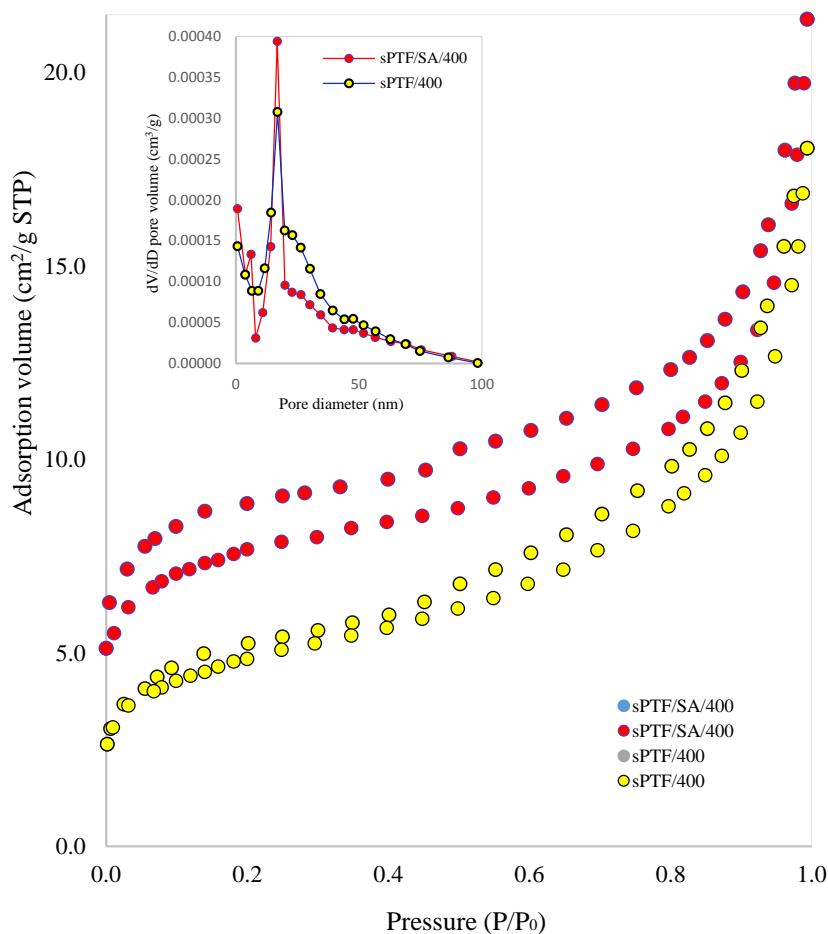


**Fig. 2.** N<sub>2</sub> adsorption-desorption isotherm and pore size distribution of sPTF/SA/400 and sPTF/400

Figure 2 also highlights the effect of adding SA to the surface properties of the mesoporous carbon materials. Both materials showed similar N<sub>2</sub> adsorption-desorption isotherm and pore size distribution curves. However, sPTF/SA/400 exhibited a larger hysteresis loop than sPTF/400 because of the thermal exchange with the SA. This could reduce the performance of sPTF/SA/400 by giving rise to complex pore structure and network effects. Conversely, the smaller hysteresis exhibited by sPTF/400 confirms the effect of only internal friction in the absence of SA. Consequently, it could be inferred from the above that the resultant large hysteresis loop could limit the catalytic activity of sPTF/SA/400

Further, FE-SEM analysis revealed large pores, sharp edges, and agglomeration on the surface of the catalysts. Figure 3a illustrates the surface microstructure of the sulfonated sPTF/SA-400 carbon catalyst as studied using FESEM. The different constituents appear to have been homogeneously processed into solid particles of varying dimensions. The EDX analysis of the surface elemental composition revealed the presence of carbon, oxygen, and sulfur (Fig. 3b).

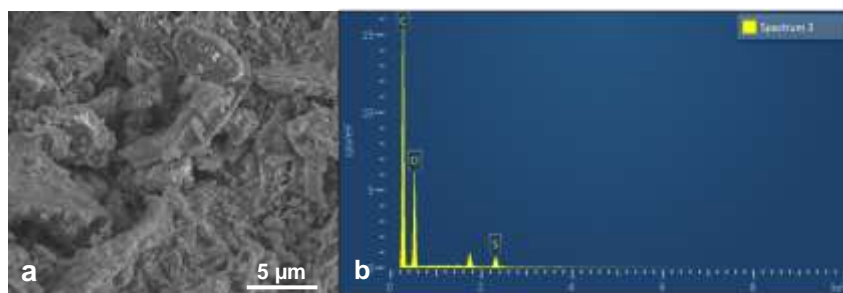


**Fig. 3.** (a) Results of the surface microstructural analysis of the sPTF/SA/400 *via* FE-SEM and (b) surface elemental composition of the sPTF/SA/400 determined *via* EDX analysis

Similarly, Fig. 4a illustrates the surface microstructure (size and shape of topographic features) of the sulfonated sPTF/SA-300 as studied using FE-SEM. The surface morphology appears to have been heterogeneously processed into solid particles into which succinic acid was not fully incorporated. The surface elemental composition (Fig. 4b) revealed the presence of carbon, oxygen, nitrogen, and sulfur. Further, FE-SEM analysis revealed large pores with sharp edges on the agglomerated catalyst surface.

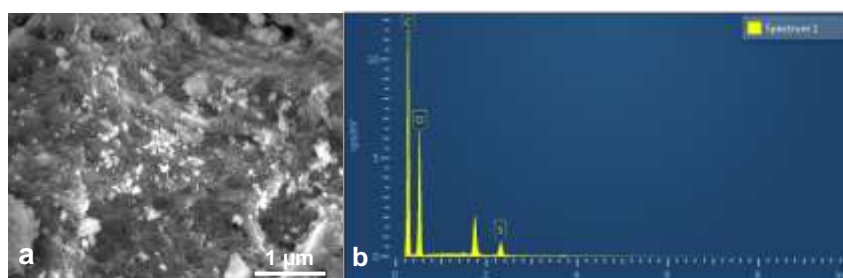


**Fig. 4.** (a) Results of the surface microstructural analysis of the sPTF/SA/300 *via* SEM and (b) surface elemental composition of the sPTF/SA/300 determined *via* EDX analysis

Figure 5a presents the surface microstructure of the sulfonated sPTS-400 carbon catalyst studied using FE-SEM. Figure 5b shows a cross-sectional surface composition and the distribution of elements on sPTS-400. The result also revealed the presence of carbon, oxygen, nitrogen, and sulfur. However, large pores with sharp edges were not evident in the FE-SEM images. The analysis indicated an agglomerated, amorphous solid with nearly uniform protrusions on its surface.

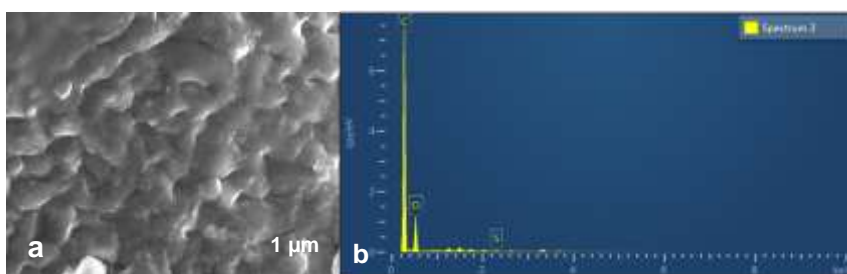


**Fig. 5.** (a) Results of the surface microstructural analysis of the sPTS-400 *via* SEM and (b) surface elemental composition of the sPTS-400 determined *via* EDX analysis



Sulfonating cellulosic materials resulted in the production of stable solids with strong acid density and many active sites. Such an approach can facilitate the synthesis of highly active catalysts from inexpensive, naturally occurring molecules. The FT-IR spectra of unsulfonated mesoporous carbon from palm tree spikelet and sulfonated catalysts are shown in Fig. 6. These results confirm the findings of Zhang *et al.* (2015) and Peng *et al.* (2010). Successful incorporation of  $-\text{SO}_3\text{H}$  groups onto the sulfonated catalysts was observed in the form of FT-IR spectrum bands in the stretching mode at  $1008\text{ cm}^{-1}$ . This vibration, attributed to symmetric S=O bonds, is absent in the spectra of unsulfonated material. It was observed that the S=O bond, represented by the peak at  $1080\text{ cm}^{-1}$ , is asymmetric. The FT-IR spectra also reveal symmetric O=S=O bonds, as shown by the vibration bands at  $1027$  and  $1167\text{ cm}^{-1}$  and those for -OH bonds at  $3424$  and  $3429\text{ cm}^{-1}$ . The node stretching at  $3440\text{ cm}^{-1}$  was assigned to the O-H stretching mode of phenolic -OH and -COOH groups. Similarly, node stretching at  $1719\text{ cm}^{-1}$  is representative of C=O bonds due to -COO- and -COOH group stretching vibrations.

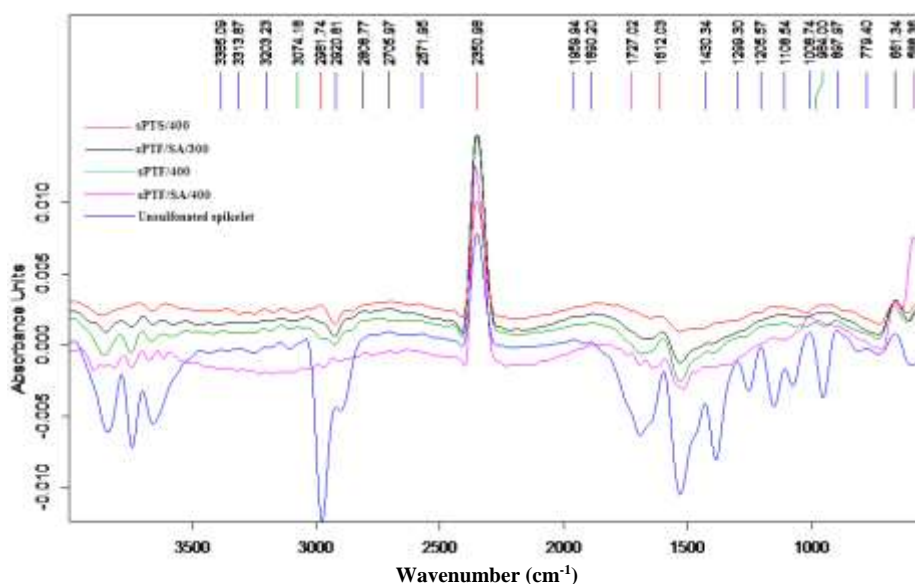


**Fig. 6.** FT-IR spectra of sPTF-300 catalysts, sPTS-400 catalysts, and unsulfonated-PTS-400 mesoporous carbon at different conditions

The aromatic C=C stretching mode, similar to graphite-like, polyaromatic materials, was ascribed to the broad, intense bands centered at  $1610\text{ cm}^{-1}$ . The effect of carbonization was observed from the disappearance of C-H stretching peaks at  $675\text{ cm}^{-1}$ ,  $700$  to  $900$ , and  $3046\text{ cm}^{-1}$ , ascribed to polycyclic aromatic and aromatic hydrocarbons, respectively. This is because the mesoporous carbon skeleton is dehydrogenated and graphitized at relatively high carbonization temperatures. Low carbonization temperature thus appears favorable in synthesizing sulfonated carbon catalysts rich in C-H bonds. This is evident from the gradual disappearance of C-H stretching peaks and the difference in the  $-\text{SO}_3\text{H}$  incorporated on sPTF/SA/400 ( $0.7851\text{ mmol/g}$ ) and sPTF/SA/300 ( $1.1283\text{ mmol/g}$ ). This is in agreement with the results of a previous report (Zhang *et al.* 2015).

### Catalytic Performance of the Solid Acid Catalysts in Biodiesel Production

The catalytic activity of the catalysts synthesized from palm frond and spikelet were evaluated. The study employed 1 wt.% catalyst loading and a methanol-to-oil molar ratio

of 5:1 within a temperature range of 100 to 200 °C. The mesoporous sulfonated solid acid catalysts exhibited high activity compared to conventional solid acid catalysts. They were able to convert a high-FFA content (48%) UFO feedstock obtained from a household in Malaysia to more than 98.51% FAMEs. Figures 7a to 7d show the catalytic activity of the sulfonated solid acid catalysts prepared under different conditions. Despite the low alcohol molar ratio, more than 80% conversion was achieved using each catalyst after 5 h reaction time. This is encouraging, considering that an 18:1 molar ratio was used in a study by Zhang *et al.* (2015), though at lower temperature.

A similar trend was observed for all reactions, with equilibrium achieved after 5 h reaction time. The highest catalytic activity (98.51% FAME) was obtained from the reaction with sPTS/400 with 1.2974 mmol/g total  $-SO_3H$  acid density. This was closely followed by sPTF/SA/300, with 1.1283 mmol/g total  $-SO_3H$  acid density.

Interestingly, despite proper sulfonation and higher surface area and pore size (27.78 m<sup>2</sup>/g and 10.02 nm), the performance of sPTF/SA/300 was slightly less than what was obtained from sPTS/400. However, it is interesting to note that mesoporosity alone does not determine the extent of catalytic activity or turnover. Other factors such as acid sites and type, acid density, carbon precursor, and crystal structure all play significant roles. This plausibly explains the reason behind the slightly lower activity of sPTF/SA-300 and sPTF/SA-400 against sPTS/400 is sPTF/400 despite possessing larger surface area,  $S_{BET}$ . Another plausible explanation is that chemical equilibrium limits the extent of esterification in isolating SA in the form of esters formed with sPTF/SA/300 (Orjuela *et al.* 2012). This probably disrupts the usual five-step Fischer-Speier esterification mechanism (Hernández-Montelongo *et al.* 2015; Aguilar-Garnica *et al.* 2014) in the presence of SA and  $-SO_3H$  acid catalysts. These steps include: increased electrophilicity on carbonyl carbon because of transfer of proton to carbonyl oxygen from acid catalyst; attack by nucleophilic oxygen atom from the methanol on the carbonyl carbon; formation of activated complex molecule as proton transfers to the second alcohol from the oxonium ion; a new oxonium ion formed from the protonation of a hydroxyl group within the activated complex; and ester produced as water is lost from the oxonium ion with consequent deprotonation (Larock 1989). To solve this problem, it is necessary to remove the product from the reacting vessel. However, the batch system employed for this study does not permit efficient product separation without further complications. Furthermore, this situation is exacerbated by hydroxyl groups formed during esterification and the low solubility and volatility of SA in methanol which requires fast esterification kinetics to avoid precipitation or accumulation in the reactor (Orjuela *et al.* 2011). Similarly, Yu *et al.* (2011) suggested acid in-excess and a stepwise addition of alcohol during the synthesis of polyester polyol. However, the performance of sPTF/SA/300 exceeded those without SA after regeneration. This signifies the beneficial effect of SA homogenization after much of the hydroxy groups have been eliminated. It also implied that both acids neither inhibit each other's rate nor compete for active sites during esterification. Again, this highlights that successful incorporation of surface strong acid density, combined with well-ordered mesoporosity, are essential for FFA conversion.

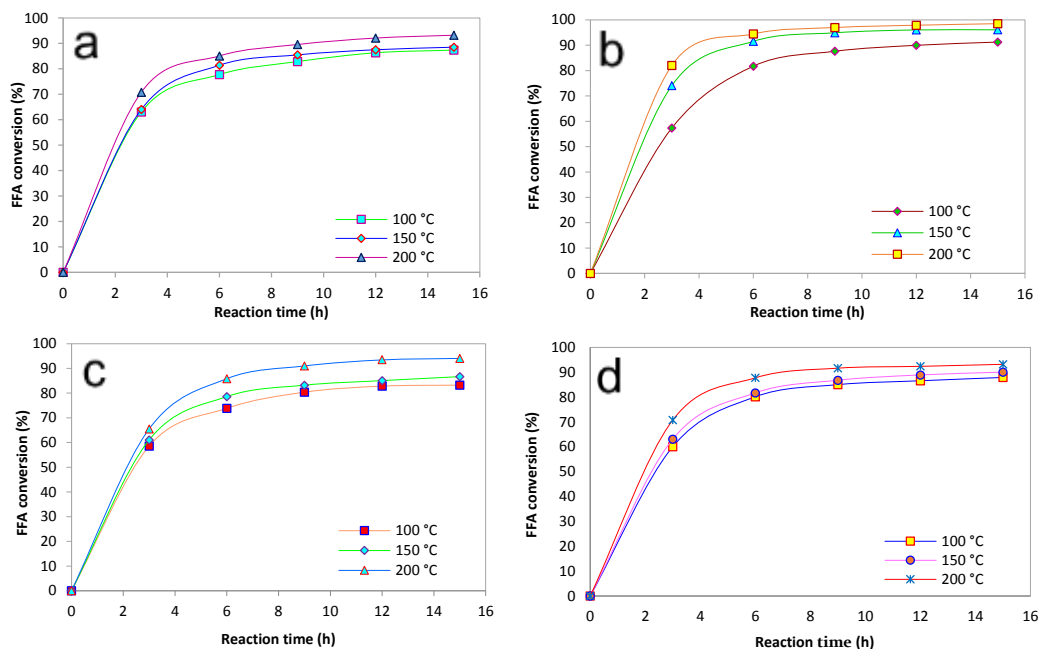


**Fig. 7.** Catalytic activities of mesoporous (a) sPTF/SA/400, (b) sPTS/400, (c) sPTF/400, and (d) sPTF/SA/300 catalysts prepared under different conditions

Further, the catalyst retained most of its activity after 8 recycles without significant leaching of its strong ( $-\text{SO}_3\text{H}$ ) groups (Fig. 8). Evidently, incorporation of strong sulfonite groups, mesoporosity, and high stability ensured the good reusability of the synthesized catalysts. Deactivation sets in as the active sites loose the strong sulfonite groups from the material after several cycles. The catalyst was regenerated by simple decantation, washing, and drying. This highlights the potential to produce alternative, environmentally benign catalysts from waste palm biomass.

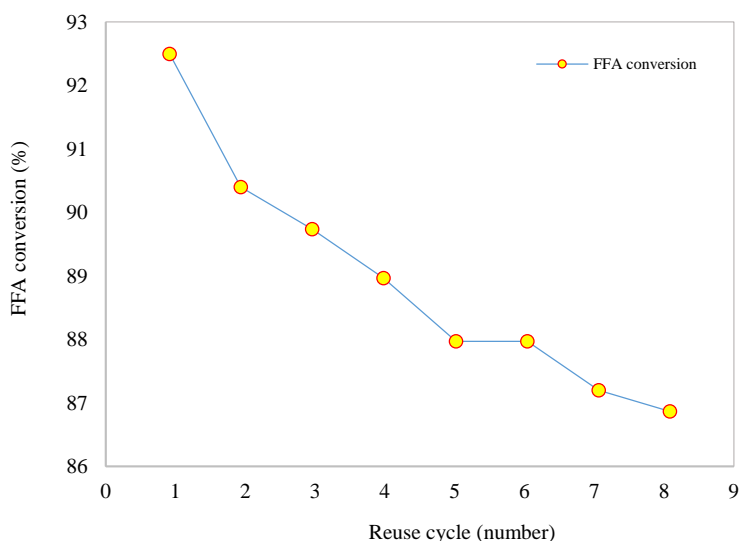


**Fig. 8.** Activity of sPTS/400 after regeneration and recycling for esterification reaction

Converting feedstocks of low economic value into high yield methyl esters shows the superiority of solid acid catalyst. In this regard, the present process is economical, as it employed moderate reaction conditions such as relatively low catalyst-loading, low temperature (100 °C), and a 5:1 alcohol-to-oil ratio to convert more than 98% high FFA feedstock. Furthermore, the deluge of waste generated from palm tree cultivation and palm oil production could be easily converted into alternative catalysts, with potential wide ranges of applications in other acid-catalyzed reactions. This is interesting when compared with other carbon-bearing solid acid catalysts. For instance, Dawodu *et al.* (2014) synthesized catalyst from the cake of *C. inophyllum* and converted 96.6 wt% of the oil extracted therefrom, which contained 18.9 wt.% FFA. This was achieved with a 30:1 methanol-to-oil molar ratio at 180 °C for 5 h and a catalyst loading of 7.5 wt.%. Similarly, Dehkhoda *et al.* (2010) obtained 92% conversion from 12.25 wt.% FFA-containing feedstock with 5 wt.% sulfonated pyrolysis biochar catalyst after 3 h under 18:1 methanol-to-oil molar ratio. It is noteworthy to mention the close to 100% conversion obtained with Ph-SO<sub>3</sub>H-modified mesoporous carbon by Geng *et al.* (2012) with 66 times more methanol than oleic acid. For a comprehensive comparison on biodiesel production from palm oil, *Jatropha curcas*, and *Calophyllum inophyllum*, the reader is referred to the article by Ong *et al.* (2011).

## CONCLUSIONS

1. Sulfonated, mesoporous carbon catalysts prepared from waste palm tree biomass with concentrated H<sub>2</sub>SO<sub>4</sub> (98%) as the sulfonating reagent converted more than 98.51% of FFA into biodiesel.
2. This study employed 400 and 150 °C carbonization and sulfonation temperatures, respectively, to avoid destroying the well-ordered mesostructure of the carbon materials, ensuring good catalytic activity by retaining high acid density on the catalysts. The catalysts in this study functioned well at the moderate process conditions of 100 °C, 5 h reaction time, 5:1 methanol-oil ratio, and 1 wt.% catalyst loading.
3. The sPTS/400 catalyst, with specific surface area 12.7037 m<sup>2</sup>/g, average pore size 10.02 nm, mesopore volume 0.02 cm<sup>3</sup>/g, and 1.2974 mmol/g total -SO<sub>3</sub>H acid density, exhibited the highest activity (98.51%). Further, it converted more than 90% of FFA after 8 consecutive regeneration cycles.
4. The observed high catalytic performance is attributed to the large pores, uniform pore size, good surface area, large mesopore volume, high -SO<sub>3</sub>H density, and hydrophobic surface of the sulfonated catalysts. The mesostructure is large enough to effectively accommodate long FFA chains. The catalysts' mesostructure makes it difficult for water molecules, either from the UFO feedstock or formed during the reaction, to access the inside of the catalysts.
5. The catalysts generated from waste biomass in this study have promise for application as solid acid catalysis and have good prospects in other acid-catalyzed reactions.

## ACKNOWLEDGMENTS

The authors are grateful for the support from HIR project number D000011-16001 for fully funding this study. We also like to acknowledge the valuable assistance in conducting characterization analyses provided by the Project No: PG144-2012B and research grants under University of Malaya, Malaysia and Tertiary Education Trust Fund (TETFund), Ahmadu Bello University, Zaria Nigeria.

## REFERENCES CITED

- Aguilar-Garnica, E. Silva-Romero, Y. E., Hernández-Montelongo, R., García-Sandoval, J. P., and Aceves-Lara, C.-A. (2014). "Kinetic analysis for the esterification of high free fatty acid feedstocks with a structural identifiability approach," *Eur. J. Lipid Sci. Technol.*, 116(11), 1598-1607. DOI: 10.1002/ejlt.201400059
- Aziz, M. A., Uemura, Y., and Sabil, K. M. (2011). "Characterization of oil palm biomass as feed for torrefaction process," *National Postgraduate Conference (NPC)*, September, IEEE. DOI: 10.1109/NatPC.2011.6136260
- Berchmans, H., and Hirata, J. S. (2008). "Biodiesel production from crude *Jatropha curcas* L. seed oil with a high content of free fatty acids," *Bioresour. Technol.* 99(6), 1716-1721. DOI: 10.1016/j.biortech.2007.03.051
- Budarin, V. L., Clark, J. H., Luque, R., and Macquarrie, D. J. (2007). "Versatile mesoporous carbonaceous materials for acid catalysed reactions," *Chem. Commun.* 22(6), 634-636. DOI: 10.1039/B614537J
- Chen, W. H., Tu, Y J., and Sheen, H. K. (2010). "Impact of dilute acid treatment on the structure of bagasse for bioethanol production," *Int. J. Energy Res.* 34(3), 265-274.
- DIN EN ISO 660. (2009). "Animal and vegetable fats and oils - Determination of acid value and acidity," *European Committee for Standardization*.
- Dawodu, F. A., Ayodele, O. O., Xin, J., and Zhang, S. (2014). "Application of solid acid catalyst derived from low value biomass for a cheaper biodiesel production," *J. Chem. Technol. Biotechnol.* 89(12), 1898-1909. DOI: 10.1002/jctb.4274
- Dehkhoda, A. M., West, A. H., and Ellis, N. (2010). "Biochar based solid acid catalyst for biodiesel production," *Appl. Catal. A.* 382(2), 197-204. DOI: 10.1016/j.apcata.2010.04.051
- Geng, L., Yu, G., Wang, Y., and Zhu, Y. (2012). "Ph-SO<sub>3</sub>H-modified mesoporous carbon as an efficient catalyst for the esterification of oleic acid," *Appl. Catal. A.* 427-428, 137-144. DOI: 10.1016/j.apcata.2012.03.044
- Ghadge, S. V., and Raheman, H. (2006). "Process optimization for biodiesel production from mahua (*Madhuca indica*) oil using response surface methodology," *Bioresour. Technol.* 97(3), 379-384. DOI: 10.1016/j.biortech.2005.03.014
- Hassan, K. B., Husin, M. A., Darus, B., and Jalani S. (1997). "An estimated availability of oil palm biomass in Malaysia," *PORIM Occasional Paper* 37, 100.
- Hassan, S. N., Sani, Y. M., Abdul Aziz, A. R., Sulaiman, N. M. N., and Daud, W. M. A. W. (2015). "Biogasoline: An out-of-the-box solution to the food-for-fuel and land-use competitions," *Energy Convers. Manage.* 89, 349-367. DOI: 10.1016/j.enconman.2014.09.050

- Hernández-Montelongo, R., García-Sandoval, J., and Aguilar-Garnica, P. E. (2015). "On the non-ideal behavior of the homogeneous esterification reaction: A kinetic model based on activity coefficients," *Reaction Kinetics, Mechanisms and Catalysis*, 1-19. DOI: 10.1007/s11144-015-0848-x
- Ishida, M., and Abu Hassan, O. (1992). "Effect of urea treatment level on nutritive value of oil palm fronds silage in Kedah," *Kelantan bulls*. 3, p. 68, in: Proceedings of the 6th AAAP Animal Science Congress, AHAT, Bangkok, Thailand.
- Janaun, J., and Ellis, N. (2011). "Role of silica template in the preparation of sulfonated mesoporous carbon catalysts," *Appl. Catal. A*. 394(1-2), 25-31. DOI: 10.1016/j.apcata.2010.12.016
- Kuo, C.-H. and Lee, C.-K. (2009). "Enhancement of enzymatic saccharification of cellulose by cellulose dissolution pretreatments," *Carbohydrate Polymers*. 77(1), 41-46.
- Larock, R. C. (1989). "Comprehensive Organic Transformations: A Guide to Functional Group Preparations," *VCH Publishers*, New York. ISBN: 9780895737106
- Liu, J. G., Wang, Q. H., Wang, S., Dexun Zou, D. X., and Sonomoto, K. (2012). "Utilization of microwave-NaOH pretreatment technology to improve performance and L-lactic acid yield from vinasse," *Biosystems Eng.* 112, 6-13.
- Liu, R., Wang, X., Zhao, X., and Feng, P. (2008). "Sulfonated ordered mesoporous carbon for catalytic preparation of biodiesel," *Carbon* 46(13), 1664-1669. DOI: 10.1016/j.carbon.2008.07.016
- Liu, T., Li, Z., Li, W., Shi, C., and Wang, Y. (2013). "Preparation and characterization of biomass carbon-based solid acid catalyst for the esterification of oleic acid with methanol," *Bioresour. Technol.* 133, 618-621. DOI: 10.1016/j.biortech.2013.01.163
- Lotero, E., Liu, Y., Lopez, D. E., Suwannakarn, K., Bruce, D. A., and Goodwin, J. G. (2005). "Synthesis of biodiesel via acid catalysis," *Ind. Eng. Chem. Res.* 44(14), 5353-5363. DOI: 10.1021/ie049157g
- Lou, W. Y., Zong, M. H., and Duan, Z. Q. (2008). "Efficient production of biodiesel from high free fatty acid-containing waste oils using various carbohydrate-derived solid acid catalysts," *Bioresour. Technol.* 99(18), 8752-8758. DOI: 10.1016/j.biortech.2008.04.038
- Maciá-Agulló, J. A., Sevilla, M., Diez, M. A., and Fuertes, A. B. (2010). "Synthesis of carbon-based solid acid microspheres and their application to the production of biodiesel," *ChemSusChem*. 3(12), 1352-1354. DOI: 10.1002/cssc.201000308
- Ong, H. C., Mahlia, T. M. I., Masjuki, H. H., and Norhasyima, R. S. (2011). "Comparison of palm oil, *Jatropha curcas* and *Calophyllum inophyllum* for biodiesel: A review," *Renew. Sustain. Energ. Rev.* 15(8); 3501-3515. DOI:10.1016/j.rser.2011.05.005
- Orjuela, A., Kolah, A., Lira, C. T., and Miller, D. J. (2011). "Mixed succinic acid/acetic acid esterification with ethanol by reactive distillation," *Ind. Eng. Chem. Res.* 50(15), 9209-9220. DOI: 10.1021/ie200133w
- Orjuela, A., Yanez-Mckay, A., Lira, C. T., and Miller, D. J. (2012). "Carboxylic acid recovery and methods related thereto," *U.S. Patent*. EP2507200 A1, Oct 10.
- Park, J. Y., Kim, D. K., and Lee, J. S. (2010). "Esterification of free fatty acids using water-tolerable amberlyst as a heterogeneous catalyst," *Bioresour. Technol.* 101(1), S62-S65. DOI: 10.1016/j.biortech.2009.03.035

- Peng, F., Zhang, L., Wang, H., Lv, P., and Yu, H. (2005). "Sulfonated carbon nanotubes as a strong protonic acid catalyst," *Carbon* 43(11), 2405-2408. DOI: 10.1016/j.carbon.2005.04.004
- Peng, L., Philippaerts, A., Ke, X., Noyen, J. V., Clippel, F. D., Tendeloo, G. V., Jacobs, P. A., and Sels, B. F. (2010). "Preparation of sulfonated ordered mesoporous carbon and its use for the esterification of fatty acids," *Catal. Today* 150(1-2), 140-146. DOI: 10.1016/j.cattod.2009.07.066
- Prauchner, M. J., and Rodríguez-Reinoso, F. (2012). "Chemical versus physical activation of coconut shell: A comparative study," *Micropor. Mesopor. Mater.* 152, 163-171. DOI: 10.1016/j.micromeso.2011.11.040
- Rabumi, W. (1998). "Chemical composition of oil palm empty fruit bunch and its ecomposition in tile field," Thesis Submitted to Universiti Putra Malaysia.
- Ramadhas, A., Jayaraj, S., and Muraleedharan, C. (2005). "Biodiesel production from high FFA rubber seed oil," *Fuel* 84(4), 335-340. DOI: 10.1016/j.fuel.2004.09.016
- Sani, Y. M., Daud, W. M. A. W., and Abdul Aziz, A. R. (2012). "Biodiesel feedstock and production technologies: Successes, challenges and prospects," in: *Biodiesel - Feedstocks, Production, and Applications*, Z. Fang (ed.), InTech, Croatia. DOI: 10.5772/52790
- Sani, Y. M., Daud, W. M. A. W., and Abdul Aziz, A. R. (2013). "Solid acid-catalyzed biodiesel production from microalgal oil - The dual advantage," *J. Environ. Chem. Eng.* 1(3), 113-121. DOI: 10.1016/j.jece.2013.04.006
- Sing, K. S. W., Everett, D. H., Haul, R. A. W., Moscou, L., Pierotti, R. A., Rouquerol, J., and Siemieniewska, T. (1985). "Reporting physisorption data for gas/solid systems with special reference to the determination of surface area and porosity," *Pure Appl. Chem.* 57, 603-619.
- Suganuma, S., Nakajima, K., Kitano, M., Kato, H., Tamura, A., Kondo, H., Yanagawa, S., Hayashi, S., and Hara, M. (2011). "SO<sub>3</sub>H-bearing mesoporous carbon with highly selective catalysis," *Micropor. Mesopor. Mater.* 143(2-3), 443-450. DOI: 10.1016/j.micromeso.2011.03.028
- Sulaiman, O. N., Salim, N. A., Nordin, R., Hashim, M., Ibrahim, M., and Sato, M. (2012). "The potential of oil palm trunk biomass as alternative source for compressed wood," *BioResources* 7(2), 2688-2706. DOI: 10.15376/biores.7.2.2688-2706
- Takagaki, A., Toda, M., Okamura, M., Kondo, J. N., Hayashi, S., Domen, K., and Hara, M. (2006). "Esterification of higher fatty acids by a novel strong solid acid," *Catal. Today* 116(2), 157-161. DOI: 10.1016/j.cattod.2006.01.037
- Toda, M., Takagaki, A., Okamura, M., Kondo, J. N., Hayashi, S., Domen, K., and Hara, M. (2005). "Biodiesel made with sugar catalyst," *Nature* 438(10), 178. DOI: 10.1038/438178a
- Veljkovic, V., Lakicevic, S., Stamenkovic, O., Todorovic, Z., and Lazic, M. (2006). "Biodiesel production from tobacco (*Nicotiana tabacum* L.) seed oil with a high content of free fatty acids," *Fuel* 85(17-18), 2671-2675. DOI: 10.1016/j.fuel.2006.04.015
- Wan Zahari, M., Mohd. Ariff, O., Mohd. Sukri, I., Oshibe, A., and Hayakawa, H. (2000). "Oil palm by-products and urea molasses mineral blocks as feed resources for buffaloes in Malaysia," in: *Proceedings of the 3rd Asian Buffalo Congress*, Kandy, Sri Lanka.

- Wang, X., Liu, R., Waje, M. M., Chen, Z., Yan, Y., Bozhilov, K. N., and Feng, P. (2007). "Sulfonated ordered mesoporous carbon as a stable and highly active protonic acid catalyst," *Chem. Mater.* 19(10), 2395-2397. DOI: 10.1021/cm070278r
- Wang, Y., Ou, S., Liu, P., Xue, F., and Tang, S. (2006). "Comparison of two different processes to synthesize biodiesel by waste cooking oil," *J. Mol. Catal. A Chem.* 252(1-2), 107-112. DOI: 10.1016/j.molcata.2006.02.047
- Wong, H. K., and Wan Zahari, M. (1997). "Nutritive value of palm kernel cake and cocoa pod husks for growing cattle," *J. Trop. Agric. Food Sci.* 25(1), 125-131.
- Xing, R., Liu, Y., Wang, Y., Chen, L., Wu, H., Jiang, Y., He, M., and Wu, P. (2007). "Active solid acid catalysts prepared by sulfonation of carbonization-controlled mesoporous carbon materials," *Micropor. Mesopor. Mater.* 105(1-2), 41-48. DOI: 10.1016/j.micromeso.2007.06.043
- Yu, T., Chang, H.-B., Lai, W.-P., and Chen, X.-F. (2011). "Computational study of esterification between succinic acid and ethylene glycol in the absence of foreign catalyst and solvent," *Polym. Chem.* 2, 892-896. DOI: 10.1039/C0PY00381F
- Yu, H., Jin, Y., Li, Z., Peng, F., and Wang, H. (2008). "Synthesis and characterization of sulfonated single-walled carbon nanotubes and their performance as solid acid catalyst," *J. Solid State Chem.* 181(3), 432-438. DOI: 10.1016/j.jssc.2007.12.017
- Zhang, J., and Jiang, L. (2008). "Acid-catalyzed esterification of *Zanthoxylum bungeanum* seed oil with high free fatty acids for biodiesel production," *Bioresour. Technol.* 99(18), 8995-8998. DOI: 10.1016/j.biortech.2008.05.004
- Zhang, M., Sun, A., Meng, Y., Wang, L., Jiang, H., and Li, G. (2015). "High activity ordered mesoporous carbon-based solid acid catalyst for the esterification of free fatty acids," *Micropor. Mesopor. Mater.* 204, 210-217. DOI: 10.1016/j.micromeso.2014.11.027
- Zong, M. H., Duan, Z. Q., Lou, W. Y., Smith, T. J., and Wu, H. (2007). "Preparation of a sugar catalyst and its use for highly efficient production of biodiesel," *Green Chem.* 9, 434-437. DOI: 10.1039/B615447F  
<http://www.bfdic.com/en/Features/Features/79.html> (Accessed on 10/03/2015)

Article submitted: December 31, 2014; Peer review completed: March 3, 2015; Revisions received and accepted: April 8, 2015; Published: April 21, 2015.  
DOI: 10.15376/biores.10.2.3393-3408